Article

"Through-Space" Nuclear Spin–Spin *J* Coupling in Tetraphosphine Ferrocenyl Derivatives: A P NMR and X-ray Structure Correlation Study for Coordination Complexes

Jean-Cyrille Hierso, Aziz Fihri, Vladimir V. Ivanov, Bernard Hanquet, Nadine Pirio, Bruno Donnadieu, Bertrand Rebire, Rgine Amardeil, and Philippe Meunier

J. Am. Chem. Soc., **2004**, 126 (35), 11077-11087• DOI: 10.1021/ja048907a • Publication Date (Web): 11 August 2004

J|A|C|S
ARTICLES
Published on Web 08/11/2004

"Through-Space" Nuclear Spin−Spin J_{PP} Coupling in Tetraphosphine Ferrocenyl Derivatives: A ^{31}P NMR and X-ray Structure Correlation Study for Coordination Complexes

Jean-Cyrille Hierso,*,† Aziz Fihri,† Vladimir V. Ivanov,† Bernard Hanquet,† Nadine Pirio,† Bruno Donnadieu,‡ Bertrand Rebière,† Régine Amardeil,† and Philippe Meunier†

Contribution from the Laboratoire de Synthèse et d'Electrosynthèse Organométalliques, UMR-CNRS 5188, Université de Bourgogne, Facultés des Sciences Mirande, 9 Avenue Alain Savary, BP 47870 F-21078 Dijon Cedex, France, and Laboratoire de Chimie de Coordination du CNRS, 256, Route de Narbonne, 31077 Toulouse Cedex 4, France

Received February 26, 2004; E-mail: jean-cyrille.hierso@u-bourgogne.fr

Abstract: Herein, we report on ^{31}P^{31}P solution-phase "through-space" nuclear spin−spin coupling constants (J_{PP}) from a novel family of organometallic tetraphosphine nickel and palladium complexes. These J_{PP} constants were accurately determined through NMR iterative simulation based on the second-order spectra obtained for the compounds. The corresponding solid-state X-ray structures of the complexes were determined, and the "through-space" P···P distances are reported. Due to the blocked conformation of the species in solution, a qualitative and semiquantitative experimental correlation is obtained, which links the geometric parameters and the intensity of the corresponding P···P coupling constant. The lone-pair overlap theory developed for ^{19}F^{19}F and ^{15}N^{19}F "through-space" couplings in organic compounds [*J. Am. Chem. Soc.* **1973**, *95*, 7747−7752; **2000**, *122*, 4108−4116] appears to be a reliable foundation on which to account for our results. Based on the reported observations, the lone-pair overlap model is extended to "through-space" ^{31}P^{31}P coupling, and the model is broadened to encompass metal orbital contributions for coordination complexes. Some of the predictions and consequences of the proposed theory are discussed.

1. Introduction

Interest in the organometallic and coordination chemistry of multidentate phosphorus-containing organic species has been ongoing for over 50 years.[1,2] New families of useful and intriguing polyphosphines are developed every year, which display interesting fundamental structural features as well as applications.[3,4]Among these new polyphosphine compounds, our group has reported on the synthesis,[5] coordination chemistry,[6] and catalytic properties[7] of the conformationally blocked ferrocenyl tetraphosphine Fc(P)$_4$^{t}Bu (1,1′,2,2′-tetrakis(diphenylphosphino)-4,4′-di-*tert*-butylferrocene, Scheme 1a). These studies have highlighted the efficiency of this triarylphosphine ligand in conjunction with palladium in Suzuki and Heck cross-coupling reactions.[7] The rotational rigidity of Fc(P)$_4$^{t}Bu, which

Scheme 1. Tetraphosphine Fc(P)$_4$^{t}Bu (a) and the Related Compound 1,1′,2,2′-Tetrakis(diphenylphosphino)-3,3′,4,4′,5,5′-hexamethylferrocene (b): General View (Top) and View from the Top (Bottom)

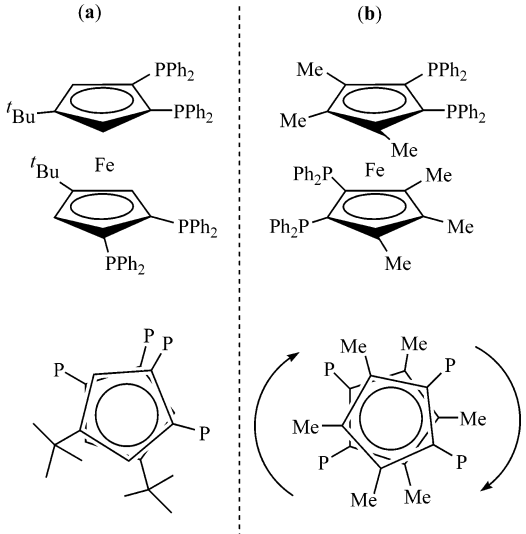

† Université de Bourgogne.
‡ Laboratoire de Chimie de Coordination du CNRS.

(1) Cotton, F. A.; Hong, B. *Prog. Inorg. Chem.* **1992**, *40*, 179.
(2) Hierso, J.-C.; Amardeil, R.; Bentabet, E.; Broussier, R.; Gautheron, B.; Meunier, P.; Kalck, P. *Coord. Chem. Rev.* **2003**, *236*, 143.
(3) For triphosphines, see: (a) Stössel, P.; Heins, W.; Mayer, H. A.; Fawzi, R.; Steimann, M. *Organometallics* **1996**, *15*, 3393. (b) Stössel, P.; Mayer, H. A.; Maichle-Mössmer, C.; Fawzi, R.; Steimann, M. *Inorg. Chem.* **1996**, *35*, 5860. (c) Stössel, P.; Mayer, H. A.; Auer, F. *Eur. J. Inorg. Chem.* **1998**, 37.
(4) For a tetraphosphine, see: (a) Feurstein, M.; Laurenti, D.; Doucet, H.; Santelli, M. *Chem. Commun.* **2001**, 43. (b) Laurenti, D.; Feurstein, M.; Pèpe, G.; Doucet, H.; Santelli, M. *J. Org. Chem.* **2001**, *66*, 1633.
(5) (a) Broussier, R.; Bentabet, E.; Amardeil, R.; Richard, P.; Meunier, P.; Kalck, P.; Gautheron, B. *J. Organomet. Chem.* **2001**, *637*−*639*, 126. (b) Broussier, R.; Ninoreille, S.; Bourdon, C.; Blaque, O.; Ninoreille, C.; Kubicki, M. M.; Gautheron, B. *J. Organomet. Chem.* **1998**, *561*, 85.
(6) Bentabet, E.; Broussier, R.; Amardeil, R.; Hierso, J.-C.; Richard, P.; Fasseur, D.; Gautheron, B.; Meunier, P. *J. Chem. Soc., Dalton Trans.* **2002**, 2322.
(7) Hierso, J.-C.; Fihri, A.; Amardeil, R.; Meunier, P.; Doucet, H.; Santelli, M.; Donnadieu, B. *Organometallics* **2003**, *22*, 4490.

Scheme 2. Complexes of Nickel and Palladium Synthesized from $Fc(P)_4{}^tBu$[a]

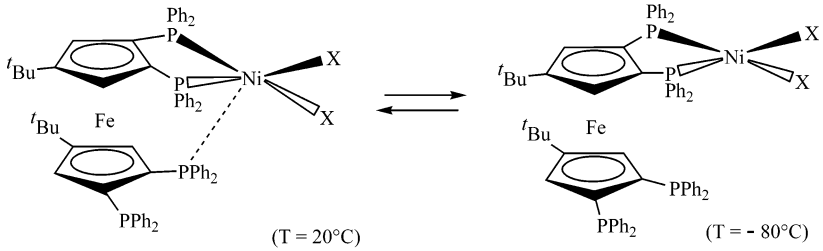

(**1**): X = Cl ; (**1b**): X = Br

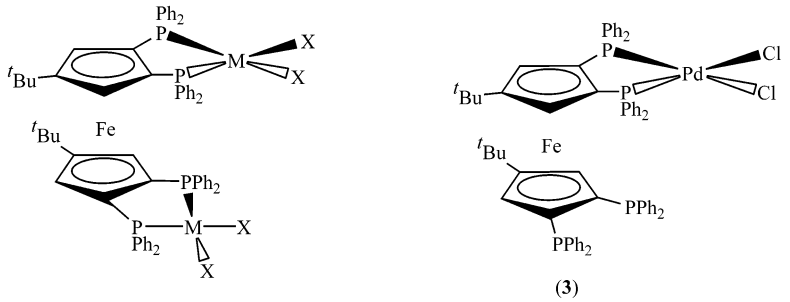

(**2**): M = Ni, X= Cl; (**2b**): M = Ni, X= Br
(**4**): M = Pd, X = Cl

(**3**)

[a] In solution, the complexes **1** and **1b** display a paramagnetic temperature-dependent behavior not detected in the ^{31}P NMR spectrum of compounds **2**, **2b**, **3**, and **4**.

has not been detected in other analogous bischelating tetraphosphines (Scheme 1b),[5b] is suspected to play an important role in its activity as an auxiliary in palladium-catalyzed reactions.[7,8] In the course of our NMR-mechanistic studies dealing with the organometallic chemistry of systems involving $Fc(P)_4{}^tBu$ and palladium allylic species, new palladium complexes (**3** and **4** in Scheme 2) with puzzling ^{31}P NMR spectra were obtained.[7] The most reasonable explanation to account for the observed NMR patterns was the existence of a variety of J_{PP} "through-space" nuclear spin−spin couplings not reported in the coordination chemistry literature up to now.

To date, the observation of "through-space" interactions has been limited to purely organic,[9] mostly fluorine-containing,[10] organic species as well as correlations based on theoretical reports.[9e,11,12]

To generate a dataset large enough to test our hypothesis concerning "through-space" interactions in coordination complexes, four novel mononuclear and dinuclear nickel complexes $[NiCl_2\{Fc(P)_4{}^tBu\}]$ (**1**) and $[Ni_2Cl_4\{Fc(P)_4{}^tBu\}]$ (**2**) (and **1b**, **2b** where bromine atoms substitute chlorines) were synthesized and fully characterized by X-ray crystallography. These extend on the previously reported $[PdCl_2\{Fc(P)_4{}^tBu\}]$ (**3**) and $[Pd_2Cl_4\{Fc(P)_4{}^tBu\}]$ (**4**) congeners.

The conformational rigidity of all of these species allows us to provide a correlation for phosphorus-containing complexes between geometric features in the solid state, and "through-space" spin−spin J_{PP} coupling constants in solution. The present work aims at completing and extending the current theory that concerns (J_{FF}) and (J_{FN}) "through-space" coupling in organic species to the (J_{PP}) spin−spin interaction in coordination compounds.

2. Experimental Section

General Considerations. All reactions and workup procedures were performed under an inert atmosphere of argon using conventional vacuum-line and Schlenk techniques. Toluene, pentane, hexane, and THF were degassed and distilled by refluxing over sodium benzophenone under argon. Dichloromethane was refluxed on calcium hydride. $CDCl_3$ and CD_2Cl_2 were degassed and stored over molecular sieves under argon prior to NMR use. Elemental analyses, ^1H (300.13 and 500.13 MHz), ^{31}P (121.49 and 202.46 MHz), and ^{13}C NMR (75.47 and 125.77 MHz), including low-temperature NMR experiments, were performed in our laboratories (respectively, on Bruker 300 and DRX 500 spectrometers).

(8) $Fc(P)_4{}^tBu$ is active as an auxiliary in Pd-catalyzed allylic amination: Urrutigoïty, M.; Hierso, J.-C.; et al., to be published.

(9) For J_{PP} coupling constants, see: (a) McFarlane, H. E. C.; McFarlane, W. *Polyhedron* **1988**, *7*, 1875. (b) McFarlane, H. E. C.; McFarlane, W. *Polyhedron* **1999**, *18*, 2117. For a J_{PSe} coupling, see: (c) Karaçar, A.; Freytag, M.; Thönnesen, H.; Omelanczuk, J.; Jones, P. G.; Bartsch, R.; Schmutzler, R. *Z. Anorg. Allg. Chem.* **2000**, *626*, 2361. For J_{PF} coupling constants, see: (d) Hughes, R. P.; Laritchev, R. B.; Williamson, A.; Incarvito, C. D.; Zakharov, L. N.; Rheingold, A. L. *Organometallics* **2002**, *21*, 4873 and ref 10h. For a general review, see: (e) Contreras, R. H.; Peralta, J. E. *Prog. Nucl. Magn. Reson. Spectrosc.* **2000**, *37*, 321.

(10) For leading references on J_{FF}, see: (a) Mallory, F. B. *J. Am. Chem. Soc.* **1973**, *95*, 7747. (b) Mallory, F. B.; Mallory, C. W.; Fedarko, M.-C. *J. Am. Chem. Soc.* **1974**, *96*, 3536. (c) Mallory, F. B.; Mallory, C. W.; Ricker, W. M. *J. Am. Chem. Soc.* **1975**, *97*, 4770. (d) Mallory, F. B.; Mallory, C. W.; Ricker, W. M. *J. Org. Chem.* **1985**, *50*, 457. (e) Mallory, F. B.; Mallory, C. W. *J. Am. Chem. Soc.* **1985**, *107*, 4816. (f) Mallory, F. B.; Mallory, C. W.; Baker M. B. *J. Am. Chem. Soc.* **1990**, *112*, 2577. (g) Mallory, F. B.; Luzik, E. D., Jr.; Mallory, C. W.; Carroll, P. J. *J. Org. Chem.* **1992**, *57*, 366. (h) Mallory, F. B.; Mallory, C. W.; Butler, K. E.; Lewis, M. B.; Xia, A. Q.; Luzik, E. D., Jr.; Fredenburgh, L. E.; Ramanjulu, M. M.; Van, Q. N.; Francl, M. M.; Freed, D. A.; Wray, C. C.; Hann, C.; Nerz-Stormes, M.; Carroll, P. J.; Chirlian, L. E. *J. Am. Chem. Soc.* **2000**, *122*, 4108 and references therein.

(11) For a review, see: (a) Contreras, R. H.; Facelli, J. C. *Ann. Rep. NMR Spectrosc.* **1993**, *27*, 255 and references therein. (b) Diz, A. C.; Contreras, R. H.; Natiello, M. A.; Gavarini, H. O. *J. Comput. Chem.* **1985**, *6*, 647. (c) Peralta, J. E.; Barone, V.; Contreras, R. H.; Zaccari, D. G.; Snyder, J. P. *J. Am. Chem. Soc.* **2001**, *123*, 9162.

(12) (a) Arnold, W. D.; Mao, J.; Sun, H.; Oldfield, E. *J. Am. Chem. Soc.* **2000**, *122*, 12164. (b) Barfield, M.; Della, E. W.; Pigou, P. E.; Walter, S. R. *J. Am. Chem. Soc.* **1982**, *104*, 3550. (c) Nakanishi, W.; Hayashi, S.; Toyota, S. *J. Org. Chem.* **1998**, *63*, 8790.

The synthesis and full characterization of the ligand Fc(P)$_4$^{t}Bu, and of the complexes [PdCl$_2${Fc(P)$_4$^{t}Bu}] (**3**) and [Pd$_2$Cl$_4${Fc(P)$_4$^{t}Bu}] (**4**), are reported elsewhere.[7]

[NiCl$_2${Fc(P)$_4$^{t}Bu}], 1. A mixture of 1,1′,2,2′-tetrakis(diphenylphosphino)-4,4′-di-*tert*-butylferrocene (855 mg, 0.83 mmol) and NiCl$_2$·DME (182 mg, 0.83 mmol) was refluxed in THF (15 mL) for 4 h. From the cooled reaction mixture, complex **1** was filtered off as an orange-red precipitate, washed with THF, and dried in vacuo (yield 762 mg, 83%). An analytically pure sample was prepared by recrystallization of the crude product from a CH_2Cl_2/hexane mixture. Anal. Calcd for $C_{66}H_{62}Cl_2P_4FeNi$ (1164.55): C, 68.1; H, 5.4. Found: C, 68.0; H, 5.2. ^{1}H NMR ($CDCl_3$): δ = 8.60−6.50 (m, 40H, Ph), 4.73, 4.67, 4.26, 4.21 (s, 1H each, Cp), 0.81, 0.71 (s, 9H each, ^{t}Bu). ^{31}P{^{1}H}($CDCl_3$, 298 K): δ = 31.8, 27.9 (m, very broad, *P*−Ni each), −18.4 (m, very broad, pendant *P*Ph$_2$), −25.9 (s, pendant *P*Ph$_2$). ^{31}P{^{1}H}(CD_2Cl_2, 193 K): δ = 33.8 (dd, J_{P1P4} = 78 Hz, J_{P1P2} = 23 Hz), 29.8 (d, J_{P4P1} = 78 Hz), −21.7 (d, J_{P2P1} = 23 Hz), −26.5 (s). ^{13}C{^{1}H}($CDCl_3$): δ = 30.8 and 31.4 (s, 1C each, ^{t}Bu*C*CH$_3$), 31.8 and 31.9 (s, 3C each, ^{t}Bu*C*H$_3$), 66.2 and 70.1 (s, 1C each, Cp*C*H,), 71.5 and 76.3 (d, 1C each, $^2J_{CP}$ = 4.5 Hz, Cp*C*H), 81.4 (d, 2C, $^1J_{CP}$ = 24 Hz, Cp*C*P), 89.2 (m, 2C, Cp*C*P), 108.8 (s, 1C, Cp*C*^{t}Bu), 118.6 (s, 1C, Cp*C*^{t}Bu), 127.0−137.0 (m, 40C, C_6H_5), 137.7, 138.6, 139.6, and 141.5 (4 m, 2C each, *ipso*-C_6H_5).

[Ni$_2$Cl$_4${Fc(P)$_4$^{t}Bu}], 2. A solution of 150 mg (0.145 mmol) of Fc(P)$_4$^{t}Bu in toluene (20 mL) was added dropwise to a suspension of NiCl$_2$·DME (62 mg, 0.28 mmol) in THF (20 mL). The mixture was stirred and heated at 90 °C for 15 h, leading to the formation of a deep red precipitate. The solvent was removed in vacuo, and the red solid was extracted with dichloromethane. After CH_2Cl_2 removal, the product was washed twice with 5 mL of hexane. Compound **2** was crystallized at −18 °C from a CH_2Cl_2/pentane mixture (yield 132 mg, 72%). Anal. Calcd for $C_{66}H_{62}Cl_4P_4FeNi_2$ (1294.15): C, 61.3; H, 4.8. Found: C, 59.9; H, 4.6. ^{1}H NMR (CD_2Cl_2): δ = 8.60−6.90 (m, 40H, Ph), 4.45 (s, 2H, Cp), 4.11 (s, 2H, Cp), 0.70 (s, 18H, ^{t}Bu). ^{31}P{^{1}H}(CD_2Cl_2): δ = 33.3 (q, J_{AB} = 76.3 Hz). ^{13}C{^{1}H}(CD_2Cl_2): δ = 30.6 (s, 6C, ^{t}Bu*C*H$_3$), 31.0 (s, 2C, ^{t}Bu*C*CH$_3$), 65.1 and 69.0 (d, 2C each, Cp*C*H, $^2J_{CP}$ = 9.0 and 12.0 Hz), 81.8 and 91.6 (dd, 2C each, Cp*C*P, $^1J_{CP}$ ≅ 48 Hz and $^2J_{CP}$ ≅ 39 Hz), 119.2 (s, 2C, Cp*C*^{t}Bu), 125.5, 126.6, 128.4, 129.4 (d, 2C each, 49 < $^1J_{CP}$ < 56 Hz, *ipso*-C_6H_5), 127.4 (d), 127.8 (d), 129.9, 130.2, 130.4 (d), 131.3, 131.8 (d), 132.2, 133.1 (d), 134.0 (d), 134.7 (d) (40C, for the doublets: 9 < $^2J_{CP}$ < 18 Hz, C_6H_5). Because of the increased solubility of complex **2** in CD_2Cl_2, and in contrast to **1b**, **2b**, and **4**, the quaternary carbons *C*P of the Cp rings could be unambiguously assigned.

[NiBr$_2${Fc(P)$_4$^{t}Bu}], 1b. A mixture of 1,1′,2,2′-tetrakis(diphenylphosphino)-4,4′-di-*tert*-butylferrocene (94 mg, 0.091 mmol) and NiBr$_2$·DME (28 mg, 0.091 mmol) was stirred in dichloromethane (60 mL) at ambient temperature for 2 h. The solution quickly turned purple. After the solution was filtered, the solvent was removed in vacuo. Upon evaporation and standing at room temperature, compound **1b** crystallized (120 mg, yield 90%), yielding single crystals suitable for X-ray studies. Anal. Calcd for $C_{66}H_{62}Br_2P_4FeNi$ (1253.45): C, 63.2; H, 5.0. Found: C, 63.3; H, 4.9. ^{1}H NMR (CD_2Cl_2): δ = 8.60−6.40 (m, 40H, Ph), 4.49, 4.14 (m, 2H each, Cp), 0.79, 0.78 (s, 9H each, ^{t}Bu). ^{31}P{^{1}H}(CD_2Cl_2, 298 K): δ = 39.2, 34.3 (m, very broad, *P*−Ni each), −23.2 (m, very broad, pendant *P*Ph$_2$), −25.7 (s, pendant *P*Ph$_2$). ^{31}P{^{1}H}(CD_2Cl_2, 193 K): δ = 39.0 (dd, J_{P1P4} = 67.0 Hz, J_{P1P2} = 31.2 Hz), 33.9 (d, J_{P4P1} = 67.0 Hz), −26.5 (d, J_{P2P1} = 31.2 Hz), −28.0 (s). ^{13}C{^{1}H}(CD_2Cl_2): δ = 29.4 and 31.0 (s, 3C each, ^{t}Bu*C*H$_3$), δ obscured for ^{t}Bu*C*CH$_3$, 65.5, 69.3, 71.8, 74.5 (m, 1C each, Cp*C*H), 127.0−135.0 (m, 40C, C_6H_5). Due to a lack of solubility, the quaternary carbons were not detected.

[Ni$_2$Br$_4${Fc(P)$_4$^{t}Bu}], 2b. A mixture of 1,1′,2,2′-tetrakis(diphenylphosphino)-4,4′-di-*tert*-butylferrocene (940 mg, 0.91 mmol) and NiBr$_2$·DME (560 mg, 1.8 mmol) was stirred and refluxed in dichloromethane (40 mL) for 15 h. The solvent of the red-purple suspension was removed in vacuo to yield compound **2b** (1.06 g, yield 80% after workup procedures). Anal. Calcd for $C_{66}H_{62}Br_4P_4FeNi_2$ (1471.95): C, 53.9; H, 4.2. Found: C, 53.6; H, 3.9. ^{1}H NMR (CD_2Cl_2): δ = 8.60−6.40 (m, 40H, Ph), 4.49 (s, 2H, Cp), 4.14 (s, 2H, Cp), 0.78 (s, 18H, ^{t}Bu). ^{31}P{^{1}H}(CD_2Cl_2): δ = 41.6 (q, J_{AB} = 65 Hz). ^{13}C{^{1}H}(CD_2Cl_2): δ = 30.6 (s, 6C, ^{t}Bu*C*H$_3$), 30.8 (s, 2C, ^{t}Bu*C*CH$_3$), 65.5 and 69.3 (d, 2C each, Cp*C*H, $^2J_{CP}$ = 8.0 and 9.0 Hz), 119.2 (s, 2C, Cp*C*^{t}Bu), 127.0−135.0 (m, 40C, C_6H_5). The lack of solubility prevents the unambiguous assignment of most of the quaternary carbons.

Cristallographic Data for Compounds 1b and 2. For compound **1b**, data were collected on a Nonius Kappa CDD (Mo Kα) diffractometer at 110 K. The structure was solved by a Patterson search program and refined by full-matrix least-squares methods based on F^2 using SHELX97 with the help of the WinGX program (Université de Bourgogne). For compound **2**, data were collected at 180 K on a IPDS STOE diffractometer (Mo Kα). The structure was solved by Direct Methods and refined by full-matrix least-squares methods based on F^2 using SHELX97 with the help of the WinGX program (LCC Toulouse).

3. Results and Discussion

With the aim of providing a more accurate interpretation of the NMR data for compounds **3** and **4** as well as the corresponding free Fc(P)$_4$^{t}Bu, we simulated the spectra.[5a,7] The simulations for Fc(P)$_4$^{t}Bu and for complex **3** are depicted in Figure 1. The corresponding numerical data are collected in Table 1, which summarizes the coupling constants obtained after iterative calculations.[13] As compared to a first-order interpretation previously reported,[5a,7] these simulations afford coupling constants with a slight deviation (0.1−3 Hz).

The same simulation procedure was applied to the newly synthesized mononuclear and dinuclear nickel complexes **1** and **2** (analogous to **3** and **4**, see Scheme 2). The bromide analogue **1b** as well as the dinuclear complex **2** (Table 2) were structurally characterized by single-crystal X-ray, thus allowing a correlation between solid-state structures (**3**,[7] **4**,[7] Fc(P)$_4$^{t}Bu,[5a] **1b**, **2**) and J_{PP} coupling constants.

3.1. NMR Spectroscopic Studies. Both chloride and bromide analogues of the mononuclear **1** and **1b** and the dinuclear **2** and **2b** display essentially identical ^{31}P NMR patterns. As compared to their palladium analogues **3** and **4**, their solution NMR spectra reveal significant differences.[7] A noticeable difference is the magnitude of the $^3J_{PP}$ coupling constants between homoannular phosphorus when compared to the dinuclear complexes [Ni$_2$Cl$_4${Fc(P)$_4$^{t}Bu}], **2**, and [Pd$_2$Cl$_4${Fc(P)$_4$^{t}Bu}], **4**. While both of these spectra confirm the presence of two pairs of isochronous phosphorus (P_1/P_2 and P_3/P_4 in Scheme 3), the signals for **2** appear at 33.73 and 32.83 ppm, J_{PP} = 76.3 Hz, as an A_2B_2 quartet, and the signals for **4** appear as a quasi doublet of doublet (almost an A_2X_2 pattern, with signals centered at 44.86 and 42.15 ppm, J_{PP} = 12.0 Hz). The discrepancy between the data obtained in solution from ^{31}P NMR between the mononuclear palladium [Pd$_2$Cl$_4${Fc(P)$_4$^{t}Bu}], **3**, and the mononuclear nickel complexes **1** or **1b** is even much more striking. The four nonequivalent phosphorus nuclei of the mononuclear compound **3** give four well-defined multiplets (Figure 1b). This suggests a 1,2-homoannular biligate coordination of the tetradentate ligand Fc(P)$_4$^{t}Bu to the palladium center (δ = 41.69, 39.24 ppm). The remaining other two homoannular phosphorus nuclei are noncoordinated (δ = −22.59, −26.34 ppm). In the case of the mononuclear nickel complex **1** (Figure

(13) The spin systems were simulated using "g-NMR" software (Adept Scientific v.-5.0). The line width was individually fitted to the experimental spectrum (see Table 1).

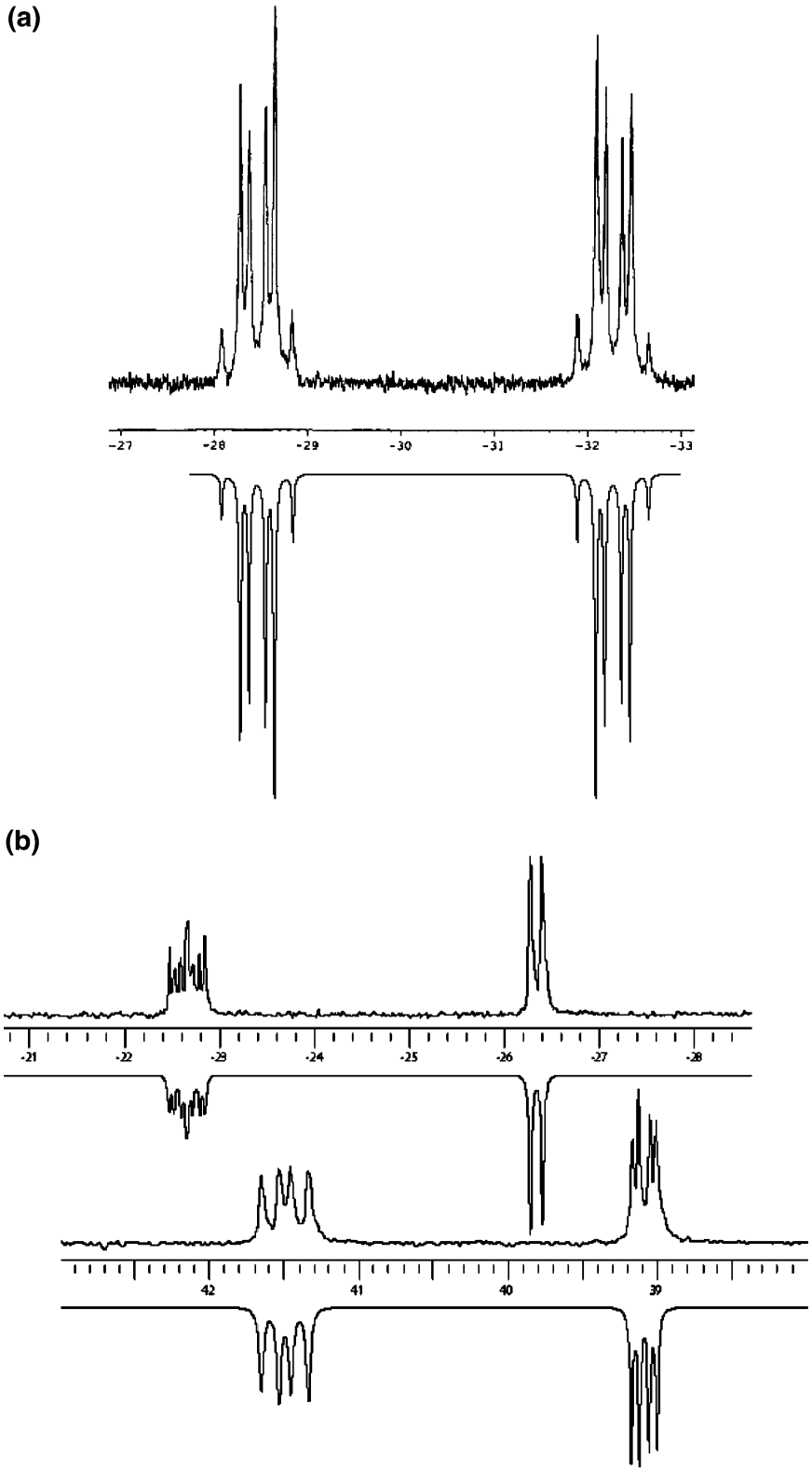

Figure 1. (a) Experimental and simulated ^{31}P NMR spectra of the ferrocenyl tetraphosphine Fc(P)$_4$^{t}Bu. (b) Experimental and simulated ^{31}P NMR spectra of the mononuclear palladium complex **3**.

2), four different phosphorus signals are observed: two at low-field ($\delta = 31.84$, 27.91 ppm) and two at high-field ($\delta = -18.45$, -25.87 ppm). At ambient temperature, the three signals at lower field are very broad ($w_{1/2} = 164$ Hz), suggesting either a fluxional behavior or a paramagnetic nickel center. The possible fluxional behavior that can be anticipated might be an equilibrium of the {$NiCl_2$}-moiety between two sites, leading to a fast intramolecular exchange from 1,2- to 1,1′-phosphorus chelating ligation. As a consequence, the resulting NMR would be an average spectrum between a diamagnetic square-planar complex and a paramagnetic tetrahedral complex.[14,15] To test this hypothesis, low-temperature ^{31}P NMR experiments were carried out. As shown in Figure 2, cooling a solution of **1** in CD_2Cl_2 transforms the three broad phosphorus signals into clearly

Table 1. Correlation of ^{31}P NMR J_{PP} Coupling Constants and X-ray Crystallographic Data ("Through-Space" Distances)

P···P distances (Å)/ coupling constant (Hz)	tetradentate compound				
	$Fc(P)_4{}^tBu$	**Pd**$Fc(P)_4{}^tBu$, **3**	**Pd**$_2Fc(P)_4{}^tBu$, **4**	$NiFc(P)_4{}^tBu$, **1b**	$Ni_2Fc(P)_4{}^tBu$, **2**
d $P_1\cdots P_2/J_{PP}$[a]	3.728(2)/59.8	3.842(1)/24.0	4.985(5)/*c*	3.644(3)/31[b]	4.987(8)/*c*
d $P_1\cdots P_3/J_{PP}$[a]	4.861(2)/*c*	4.698(2)/*c*	5.372(5)/*c*	5.397(3)/*c*	5.382(8)/*c*
d $P_4\cdots P_2/J_{PP}$[a]	4.861(2)/*c*	4.440(1)/6.4	5.351(4)/*c*	4.429(3)/*c*	5.373(9)/*c*
d $P_4\cdots P_3/J_{PP}$[a]	6.633(2)/*c*	6.292(2)/*c*	6.582(5)/*c*	6.740(3)/*c*	6.577(8)/*c*
d $P_1\cdots P_4/J_{PP}$[a]	3.364(2)/74.5	3.035(2)/15.7	3.113(5)/13.0	3.002(3)/67[b]	2.950(7)/76.3
d $P_2\cdots P_3/J_{PP}$[a]	3.364(2)/74.5	3.515(2)/14.3	3.018(5)/13.0	3.765(3)/*c*	3.067(7)/76.3

[a] Values from simulated spectra at ±0.1 Hz, except for **3** at ±0.5 Hz and **1b** at ±1 Hz. [b] J_{PP} values are given at −80 °C due to the broadening from the paramagnetic influence observed at ambient temperature (Figure 2); the data are from compound **1b**, that displays a temperature-dependent ^{31}P NMR spectrum similar to that of **1**.[17] [c] Coupling constant null or <0.5 Hz. The numbering scheme corresponds to that displayed in Scheme 3.

Scheme 3. Representation of the Complexes and Phosphorus Numbering (P_x) Used in the Discussion

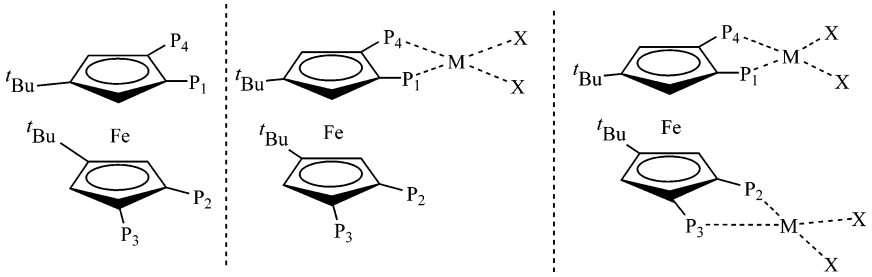

identifiable multiplets. This phenomenon is fully reversible upon warming to room temperature. Only very weak shifts of the signals are observed (≤4 ppm) between 298 and 193 K. If two magnetically different species (a paramagnetic tetrahedral and one diamagnetic square-planar complex) were in equilibrium, we expect a significant change in chemical shift upon cooling, which is clearly not the case.

The alternative explanation implies a weakly bonding interaction between the phosphorus P_2 and the nickel center to yield a 4 + 1 coordination. This leads to a structural distortion of the square-planar (diamagnetic) environment to afford an elongated pseudo-five-coordinate geometry (see Scheme 2, top). Comparable elongated five-coordinate geometries have been reported for nickel(II)/trisphosphine complexes.[16] Furthermore, it explains why the P_2 signal appears at high-field (as compared to Ni-bonded P_1 and P_4) and yet is broadened. This weak interaction between the phosphorus P_2 and the paramagnetic nickel center (leading to a broadened signal) at ambient temperature disappears upon cooling to 193 K, to yield a sharp ^{31}P NMR signal, indicative of a square-planar diamagnetic Ni(II) coordination (Figure 2).[17]

At 193 K, the ^{31}P NMR spectrum of the mononuclear complex **1** can be described as a first-order ABMX spin system with detectable coupling constants between P_1/P_4 and P_1/P_2. In contrast to P_2, its P_3 neighbor appears at all temperatures as a sharp singlet. This suggests that this donor is fully decoupled (chemically and magnetically) from the rest of the system.

To confirm the structural assumptions deduced from the low-temperature NMR evidence, the X-ray structural determination of the mononuclear nickel compound **1b** (as well as the dinuclear nickel complex **2**) was carried out.

3.2. Crystallographic Studies. The X-ray structure obtained for **1b** (Figure 3) is consistent with the NMR spectra observed in solution at low temperature for the mononuclear nickel complexes **1** and **1b**. The nickel center lies in a slightly distorted square-planar environment, and while two phosphorus atoms are bonded to Ni, two other homoannular phosphorus atoms remain pendant.

As compared to the molecular structure of the palladium analogue **3**,[7] the cyclopentadienyl planes show a smaller deviation from an eclipsed conformation: 9.7(6)° for **1b** versus 17.1(6)° for **3** (mean value of dihedral angles defined by C(1i)−CNT(1)−CNT(2)−C(2i), C(1i) and C(2i) being atoms of both Cp rings). An additional difference is the heteroannular phosphorus−phosphorus internuclear distances (see Table 1 and Scheme 3): for **1b**, the P_2 is closer to P_1 and P_4, while P_3 is significantly further from P_1 and P_4 (d $P_1\cdots P_3$ = 5.397(3) Å against 4.698(2) Å for **3**, d $P_4\cdots P_3$ = 6.740(3) Å against 6.292(2) Å for **3**). Thus, in **1b**, one of the pendant phosphorus atoms (P_3) is clearly isolated from the first coordination sphere of the nickel.[18] These results are in full agreement with the following:

i) the ^{31}P NMR spectrum of **1b** which shows, at all considered temperatures, the most shielded signal for P_3 as a singlet which does not undergo any paramagnetic influence (similar to the phenomenon depicted in Figure 2 for **1**), and

ii) the possibility, at the higher temperature and in solution, of an elongated pseudo-five-coordinate complex formation involving the atom P_2 (Scheme 3, middle).

Comparing the homoannular P···P distances, we note a significant difference for the d $P_2\cdots P_3$ between the free ligand $Fc(P)_4{}^tBu$, and the corresponding mononuclear palladium and nickel analogues **3** and **1b** (3.364(2), 3.515(2) Å vs 3.765(3)

(14) Angulo, I. M.; Bouwman, E.; Lok, S. M.; Lutz, M.; Mul, W. P.; Spek, A. L. *Eur. J. Inorg. Chem.* **2001**, 1465.
(15) 1,1′-P(Ph_2) bound nickel halide complexes of ferrocenyl diphosphine ligands display a tetrahedral geometry: (a) Butler, I. R.; Cullen, W. R.; Kim, T.-J.; Rettig, S. J.; Trotter, J. *Organometallics* **1985**, *4*, 972. (b) Casellato, U.; Ajo, D.; Valle, G.; Corain, B.; Longato, B.; Graziani, R. *J. Crystallogr. Spectrosc. Res.* **1988**, *18*, 583.
(16) Benelli, C.; Di Vaira, M.; Noccioli, G.; Sacconi, L. *Inorg. Chem.* **1977**, *16*, 182 and references therein. Longer metal−ligand distances (radial expansion) are predicted and found in five-coordinate high-spin complexes, as compared to low-spin complexes.
(17) The ^{31}P NMR spectrum at −80 °C for **1b** is available as Supporting Information.
(18) The wide *exo*-open angles P(3)−C(35)−C(36) = 130.0(5)° and P(4)−C(36)−C(35) 127.0(5)° (see Figure 3) should also be noted, while in the other X-ray structures of **2**, **3**, **4**, and $Fc(P)_4{}^tBu$, the corresponding angles display values ≤120°.

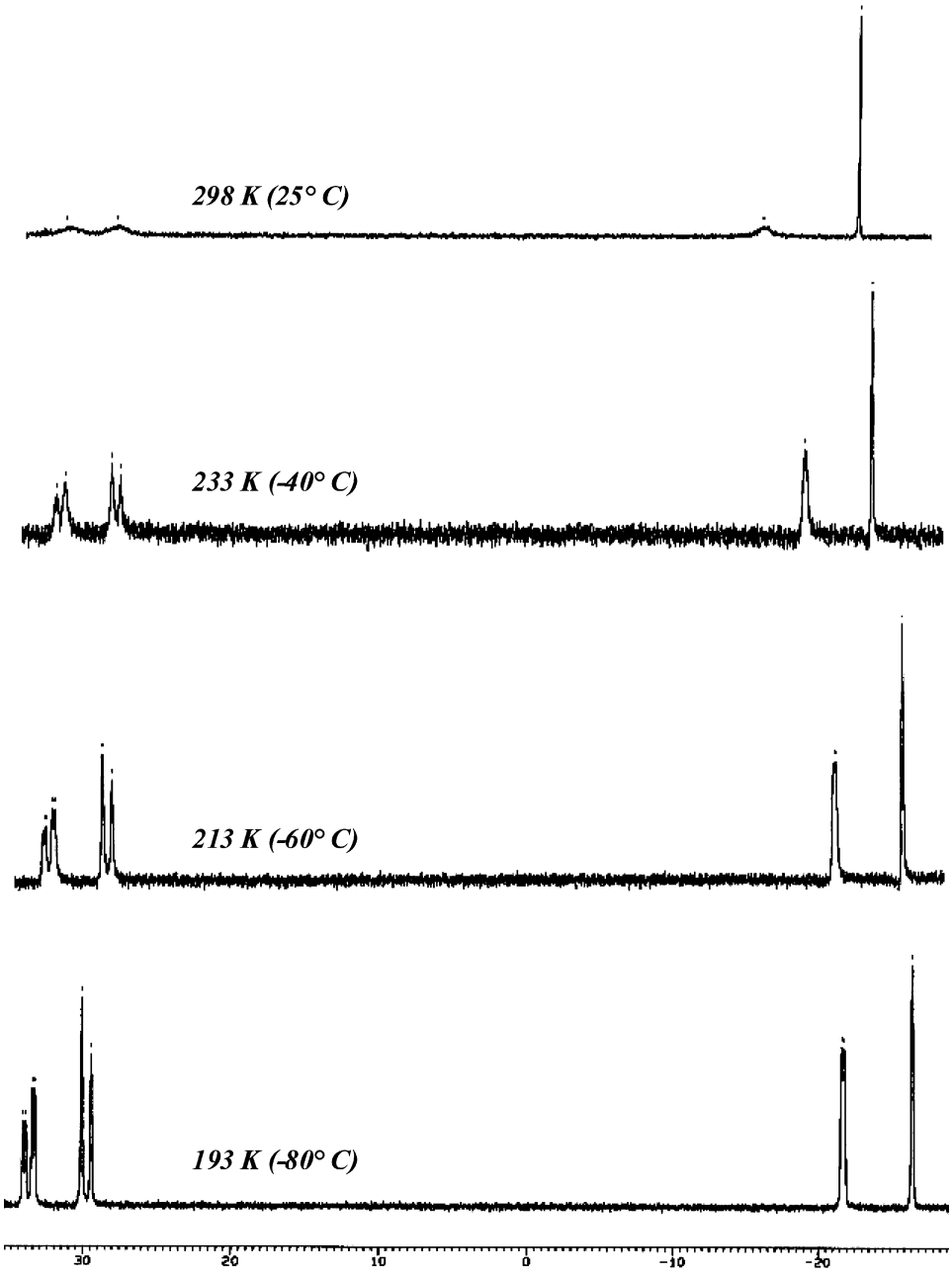

Figure 2. Variable-temperature ^{31}P NMR monitoring of the mononuclear nickel complex **1**.

Å, respectively). Interestingly, the only system which displays no P_2 P_3 coupling constant is the nickel complex **1b**.

The X-ray structure obtained for **2** (Figure 4) and compared to that obtained for the congener dinuclear palladium complex **4**[7] indicates quasi similar structures for **2** and **4**. The Cp planes show deviations from an eclipsed conformation of 12.2(6)° and 13.1(3)°, respectively, and the phosphorus−phosphorus heteroannular internuclear distances are equal in the range of ±0.02 Å (see Table 1). The need to rationalize the J_{PP} results summarized in Table 1 led us to propose the theoretical model described in the following.

3.3. Model for Nonbonded Spin−Spin Coupling Interactions. Organic compounds containing pairs of fluorine atoms (or nitrogen/fluorine atoms) that are intramolecularly crowded against one another exhibit large $^{19}F^{19}F$ (or $^{19}F^{15}N$) nuclear spin coupling constants J_{FF} or J_{FN}.[10] This phenomenon commonly designated as "through-space" coupling (also called nuclear spin−spin coupling via nonbonded interactions) has been analyzed by Mallory and co-workers using a simple but powerful perturbation model. The "through-space" couplings result from overlap interactions between lone-pair orbitals on the two crowded elements. For instance, in the particular constrained geometry of the compounds sketched in Scheme 4 (top), the C−F/C−F, or C−F/C−N bonds, are coplanar and approximately parallel. As a consequence, the nonbonding distances *d* F···F, or *d* F···N, are short. In this orientation, the two lone-pair orbitals experience a σ-directed overlap. As displayed in Scheme 4 (bottom), the overlap between these lone-pair orbitals is expected to afford an in-phase and out-of-phase combination. As both orbitals are occupied (two-orbital, four-electron interaction), no stabilization is observed. However, it provides an adequate pathway for transmitting spin information between the

Table 2. Crystal Data, Data Collection, and Structure Refinements for Compounds **1b** and **2**

	1b·$3CHCl_3$	**2**·CH_2Cl_2
formula	$C_{66}H_{62}Br_2P_4FeNi·3CHCl_3$	$C_{67}H_{64}Cl_6P_4FeNi_2$
formula weight	1611.52	1379.03
temperature, K	110(2)	180(2)
crystal color	purple	red
crystal system	monoclinic	monoclinic
space group	$P2_1/n$	$P2_1/n$
a, Å	12.1064(2)	14.3226(19)
b, Å	40.2368(7)	22.814(3)
c, Å	14.5029(3)	21.159 (3)
β, deg	93.320(1)	104.850(14)
volume, Å^3	7052.8(2)	6682(15)
Z	4	4
calculated density, mg m^{-3}	1.518	1.371
absorption coeff., mm^{-1}	2.078	1.146
F(000)	3264	2840
θ range for data collection	2.47−26.06°	2.5−45.0°
reflections collected/unique	26 492/12 660	26 546/7872
R(int)	0.0931	0.2225
refinement method	full-matrix least-squares on F^2	
goodness-of-fit on F^2	1.014	0.826
final *R* indices [$I > 2\sigma(I)$]	R1 = 0.0691, wR2 = 0.1278	R1 = 0.0840, wR2 = 0.1915
R indices (all data)	R1 = 0.1668, wR2 = 0.1583	R1 = 0.2161, wR2 = 0.2609
residuals, e Å^{-3}	1.390, −1.557	0.726, −0.424

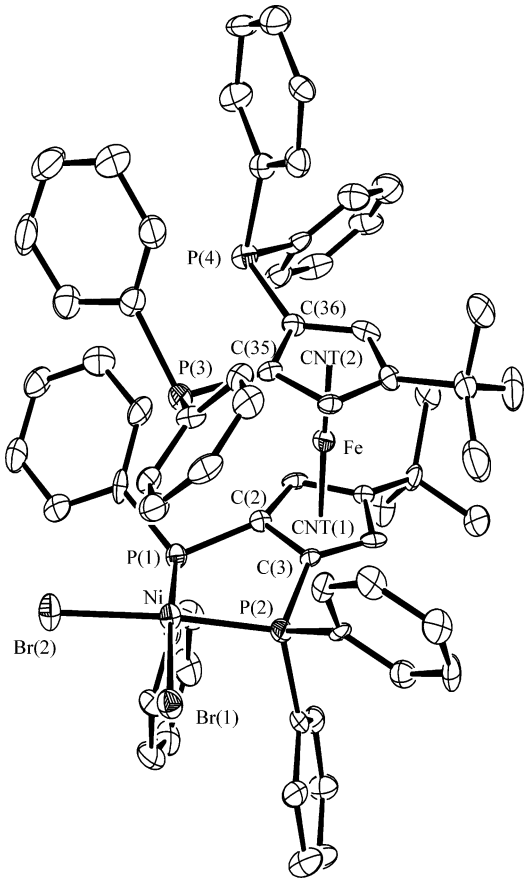

Figure 3. Plot of the molecular structure of **1b**. Selected bond lengths (Å) and angles (deg): Fe−CNT(1) 1.688, Fe−CNT(2) 1.687, Ni−P(1) 2.187(2), Ni−P(2) 2.173(2), Ni−Br(1) 2.3548(11), Ni−Br(2) 2.3379(11); CNT(1)−Fe−CNT(2) 177.77, P(2)−Ni−P(1) 87.01(7), P(1)−Ni−Br(2) 89.63(6), P(2)−Ni−Br(1) 89.05(6), Br(2)−Ni−Br(1) 93.33(4), P(3)−C(35)−C(36) 130.0(5), P(4)−C(36)−C(35) 127.0(5), P(1)−C(2)−C(3) 114.4(4), P(2)−C(3)−C(2) 117.0(5).

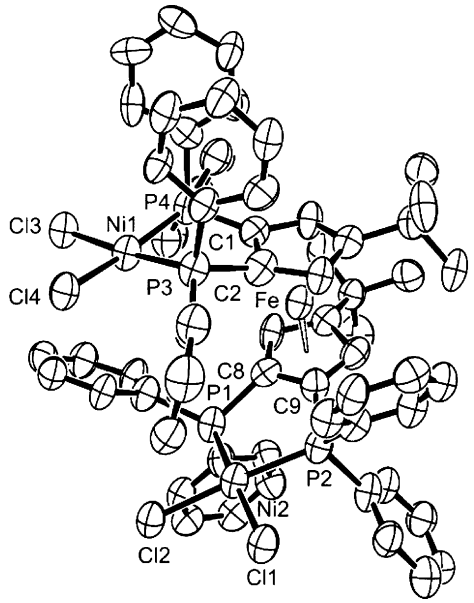

Figure 4. Plot of the molecular structure of **2**. Selected bond lengths (Å) and angles (deg): Fe−CNT(1) 1.687, Fe−CNT(2) 1.671, Ni(1)−P(3) 2.161(6), Ni(1)−P(4) 2.147(5), Ni(2)−P(1) 2.160(5), Ni(2)−P(2) 2.182(6), Ni(1)−Cl(1) 2.187(5), Ni(1)−Cl(2) 2.195(5), Ni(2)−Cl(3) 2.194(5), Ni(2)−Cl(4) 2.201(5); CNT(1)−Fe−CNT(2) 173.49, P(1)−Pd(1)−P(3) 84.40(10), P(3)−Pd(1)−Cl(2) 89.87(10), P(1)−Pd(1)−Cl(1) 91.48(10), Cl(2)−Pd(1)−Cl(1) 93.70(10), P(2)−Pd(2)−P(4) 87.41(10), P(4)−Pd(2)−Cl(4) 91.00(10), P(2)−Pd(2)−Cl(3) 90.95(11), Cl(3)−Pd(2)−Cl(4) 90.45(11), C(23)−C(24)−P(1) 118.1(7), C(13)−C(14)−P(2) 116.5(7), C(24)−C(23)−P(3) 113.4(7), C(14)−C(13)−P(4) 118.8(8).

coupled nuclei. The magnitude of J_{FF} depends on the extent to which the two lone-pair orbitals interact due to their overlap.

This model, initially mainly qualitative,[10a,g] has led to a breakthrough when the so-called overlap interaction has been quantitatively estimated for a family of 1,8-difluoronaphthalene through an exponential relation between the ab initio calculated internuclear distances and the J_{FF} coupling observed.[10h]

On the basis of this excellent work exclusively dealing with organic species and (FF) nuclear spin coupling, we propose to extend this model to phosphorus nuclear $^{31}P-^{31}P$ spin−spin "through-space" interactions and to complete it with the case of metallo-organic species.

3.3.1. The Problem of "Through-Space" versus "Through-Bond" Nuclear Coupling in the Case of Multidentate

Scheme 4. Bonding and Anti-Bonding Orbitals Generated by the Overlap of Two Lone-Pair Orbitals on Intramolecularly Crowded Nitrogen- and Fluorine-Containing Compounds

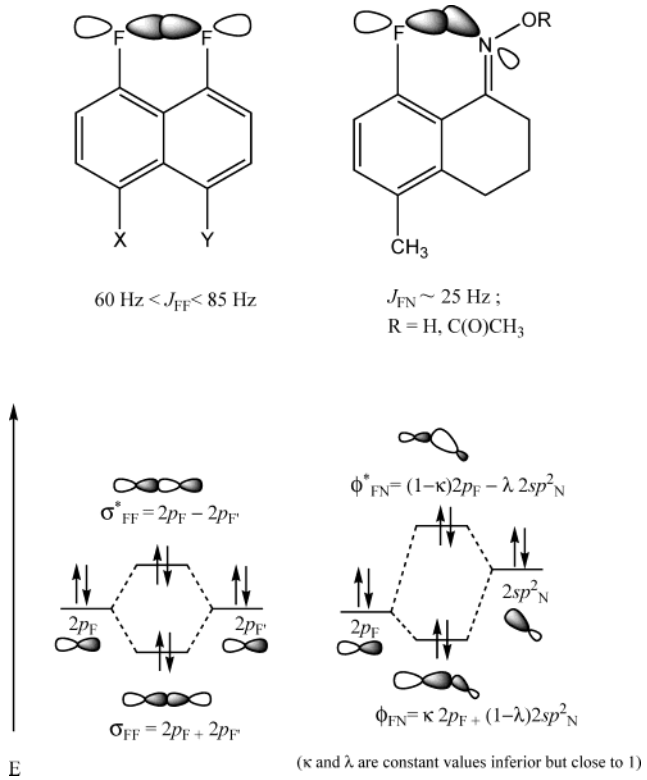

Phosphinoferrocene Compounds. In the general approach used to describe the origin of nuclear spin coupling constants, the three terms of eq 1 are distinguished:

$$J_{XX'} = {}^{ts}J_{XX'} + {}^{tb(\pi)}J_{XX'} + {}^{tb(\sigma)}J_{XX'} \qquad (1)$$

The coupling constant term ${}^{ts}J_{XX'}$ is due to "through-space" interaction, and the two other terms ${}^{tb}J_{XX'}$ arise from "through-bond" interaction (σ- and π-transmitted components).[10h,11a] The common scheme to experimentally evaluate strong ${}^{ts}J_{XX'}$ is to study systems where the shortest "through-bond" pathway is long enough (at least four bonds) that one could reasonably assume that "through-bond" contributions to nuclear coupling are negligible in magnitude. In the case of the tetraphosphine ferrocenyl derivatives presented here, the shortest "through-bond" interactions between phosphorus couples can be considered as ${}^3J_{PP'}$ coupling constants for homoannular phosphorus, and ${}^4J_{PP'}$ for heteroannular phosphorus couples (for instance, $P_1-C-Fe-C-P_2$ or $P_1-C-Fe-C-P_3$, Scheme 3). The ^{31}P NMR spectra of all of the studied compounds display no detectable values for J_{P1P3} (entry 2 in Table 1). This suggests that both ${}^{ts}J_{P1P3}$ and "through-bond" ${}^4J_{P1P3}$ are too small to be detected. In contrast, J_{P1P2} shows values ranging from 0 to 60 Hz (entry 1 in Table 1), while there is no valid argument to account for the fact that the "through-bond" ${}^4J_{P1P2}$ coupling should be different from ${}^4J_{P1P3}$ found (because the "through-bond" environments of P_2 and P_3 are identical). Thus, due to the particular geometry of these tetraphosphine species, it can be ascertained that heteroannular coupling is exclusively arising from "through-space" interactions and that "through-bond" ${}^{4tb}J_{PP'}$ contributions are nondetectable. The case of homoannular ${}^3J_{PP'}$ is more delicate and is discussed in section 3.3.3.

3.3.2. The Requirements for "Through-Space" Nuclear Spin−Spin Coupling. Empirical requirements for the detection of true "through-space" coupling constants can be derived from the last 30 years of work concerning mainly (FF),[10a,b,f,h] (NF),[10e,g] (HF), or (CF)[10c,d] spin−spin coupling, and occasionally (PX),[9a−d,10h] with X = P, Se, F. The first requirement is trivial but involves in practice some "architectural" difficulties. To easily and directly detect a coupling constant when the nuclei are of same nature, they have to be anisochronous. The molecule must be dissymmetric (see Scheme 4, top left). That is mainly why so few "through-space" (PP) couplings have been reported to date.[19,20] The second requirement is that the nuclei must be in close proximity in solution. A way to achieve this is to provide backbone rigidity: this is the case of Mallory and coworkers' aromatic-fluorine species.[10] That is the case, as well, of the polymetallic catenanes-containing bridging phosphorus reported by Rheingold and Fountain.[19] This conformational rigidity is also evoked by Ito et al. in their diphosphine bis-(ferrocenyl) compounds.[20] In our case as well, the tetraphosphine species described here have a locked-conformation in solution even at temperatures above 70 °C.[5a,7] A last requirement invoked by Mallory is the presence of two lone-pair atomic orbitals for mutual overlap.

3.3.3. Extension of the Lone-Pair Overlap Interaction Model and Involvements. In the case of the ferrocenyl tetraphosphine $Fc(P)_4{}^tBu$ (Scheme 5, top), the spatial proximity of the two heteroannular phosphorus P_1 and P_2 atoms (Scheme 3) and their lone-pair spatial orientation (ascertained by X-ray diffraction study[5a]) certainly lead to an $3sp^3-3sp^3$ orbital overlap of the same nature as those assumed for 2p−2p orbitals in F/F pairs or for $2p-2sp^2$ orbitals in F/N pairs (Scheme 4). In line with Mallory's theory,[10] the overlap of phosphorus lone-pair atomic orbital might be formulated as generating two molecular orbitals occupied by four electrons. That overlap interaction does not lead to net chemical bonding between the phosphorus atoms but ensures the transmittal of nuclear spin information. As has been detailed for fluorine atoms,[10a] the overlap between the electronic clouds generates significant Fermi contact (FC) interactions[12a] between the P nuclei.

In agreement with this simple, but powerful model, recent theoretical work has shown that a neat distinction should be made between the "through-space" transmission of the FC term and of the paramagnetic spin−orbit (PSO) terms.[21a,b] The predominant role of the Fermi contact has been confirmed by density functions interpretation,[21c] some specifically addressing the problem of "through-space" J_{FF} coupling.[12a] In the present J_{PP} coupling, as demonstrated in the case of F···F interactions, the magnitude of the coupling between two crowded phosphorus

(19) As a rare example, see: Rheingold, A. L.; Fountain, M. E. *Organometallics* **1984**, *3*, 1417. In this work, a ${}^2J_{P\cdots P}$ of 125.4 Hz was found and correlated to the internuclear "through-space" distance $d(P\cdots P) = 2.715(3)$ Å; the authors underline the lack of sufficient NMR and crystallographic data to demonstrate the extent and nature of correlations between $d(P\cdots P)$ and ${}^2J_{P\cdots P}$. It might be added that, in ${}^2J_{P\cdots P}$ cases, the relative contribution of ${}^{ts}J_{PP'}$ and ${}^{tb}J_{PP'}$ is difficult to estimate.

(20) As a rare example, see: Sawamura, M.; Hamashima, H.; Sugawara, M.; Kuwano, R.; Ito, Y. *Organometallics* **1995**, *14*, 4549. In this work, a ${}^7J_{P\cdots P}$ of 22.0 Hz has been found; unfortunately, no X-ray structural data are reported. This value was found for the only dissymmetric derivative (containing PPh_2 and $P(p\text{-Tol})_2$ moieties) of a family of diphosphine bis-(ferrocenyl) compounds.

(21) (a) Soncini, A.; Lazzeretti, P. *J. Chem. Phys.* **2003**, *118*, 7165. (b) Wu, A.; Gräfenstein, J.; Cremer, D. *J. Phys. Chem.* **2003**, *107*, 7043. (c) Soncini, A.; Lazzeretti, P. *J. Chem. Phys.* **2003**, *119*, 1343.

Scheme 5. Extension of the Lone-Pair Overlap Interaction Model to Phosphorus Atoms (Left), and Schematic Diagram Applied to Coordination Complexes Involving a Transition Metal Orbital Contribution (Right)

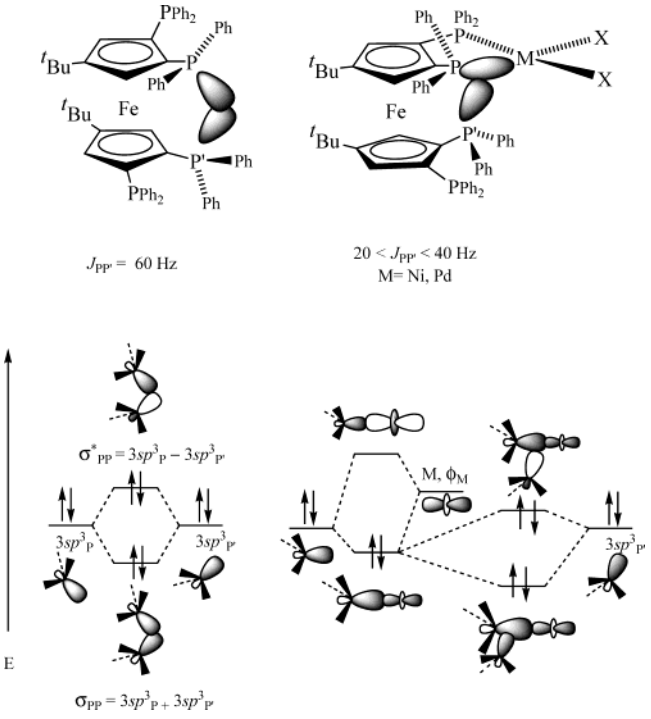

that each bear a lone-pair depends on the effectiveness of the overlap interactions between the two lone-pair orbitals.

Interestingly, in the mononuclear Pd and related Ni complexes **3** and **1b**, one of the two "through-space" interacting phosphorus lone-pairs is involved in P−M bonding interactions. Thus, the "through-space" interaction involves a three-center system composed of P−M (M = Ni, Pd) and P. Scheme 5 (right) presents an important corollary to the model developed for fluorinated purely organic compounds. For simplicity, only the three localized orbitals involved in the "through-space" interaction are sketched in Scheme 5. The metal−ligand bond between P_1 and M is considered as coming from the σ-overlap between a $3sp^3$ and a d_{z^2} orbital.[22] To account for the fact that nuclear spin information is transmitted between the phosphorus atoms, two filled molecular orbitals have been constructed which incorporate a contribution from the metal. The qualitative orbital ordering as well as the symmetry of the interacting orbitals allow this schematic view. Consequently, to observe "through-space" nuclear spin coupling, two lone-pair orbitals are not required. One lone-pair orbital with an appropriate orientation can interact with a bonding electron pair shared between a phosphorus and a metal and thus transmit "through-space" nuclear spin P···P information.

In light of the above model, the results summarized in Table 1 are examined below.

3.4. Discussion of the Model Applied to Tetraphosphine Ferrocenyl Derivatives.

3.4.1. Heteroannular Coupling in Metal Complexes. As was explained in section 3.3.2, the heteroannular phosphorus coupling constants exclusively arise from nonbonded interactions. From the 20 results of heteroannular PP′ coupling constants observed (entries 1−4), it clearly appears that the values of $J_{PP'}$ present a strong inverse dependence on P···P distances. Whatever the compound, for P···P distances above 4.90 Å, no detectable $J_{PP'}$ is observed. On the other hand, for distances below 4.00 Å, $J_{PP'} > 20$ Hz are systematically obtained.

No heteroannular phosphorus coupling constants are detected for the dinuclear metal complexes **2** and **4**. As none of the phosphorus atoms possess a lone-pair for overlap interactions, a "through-space" interaction for such a situation would require an overlap between two bonding orbitals (rather than a lone-pair and a bonding orbital). Such a situation awaits experimental demonstration. In line with the absence of orbital interactions, the phosphorus center distances lie in the range between 4.98 and 6.58 Å.

More specifically, the phosphorus distances (d P_4···P_2) are comparable in the nickel complex **1b** and in the related palladium complex **3** (∼4.4−4.3 Å within the range of standard deviation). However, the palladium complex **3** exhibits a J_{P2P4} = 6.4 Hz, whereas the nickel complex **1b** displays no such heteroannular "through-space" coupling. This is consistent with the proposed theoretical extended-formulation involving a metal-orbital contribution. As the extent of the palladium valence orbital is larger than its nickel analogue, the extent of an effective overlap with the lone-pair orbital is larger, thus yielding a detectable "through-space" coupling constant between the phosphorus nucleus. The proposed model allows one to predict that, in an analogous case involving a platinum mononuclear species, for instance, at a similar distance (d P···P), a coupling constant P_2P_4 would most probably be detected.

3.4.2. Homoannular Coupling in Complexes. In the case of homoannular coupling (entries 4 and 5), the situation is more complicated because $J_{PP'}$ is the sum of two terms $^{ts}J_{PP'} + {}^{3tb}J_{PP'}$. The contribution from "through-bond" $^{3tb}J_{PP'}$ could be nonnegligible (or even of inverse algebraic sign relative to $^{ts}J_{PP'}$).[11c] Moreover, an eventual nonbonding interaction between two filled orbitals would no longer occur via an interaction of mainly axial nature (as described for heteroannular phosphorus sp^3 orbitals) but more of lateral symmetry, and thus of weaker overlap effectiveness. The results in Table 1 (entries 4 and 5) suggest that the contribution of a nonbonded lateral σ-type interaction between the homoannular phosphorus atoms for the palladium complexes **3** and **4** would be very weak because, for distances ranging from 3.019 to 3.515 Å, very similar coupling constants of moderate intensity are found (∼14 Hz). We thus propose that, in the case of the palladium species, the homoannular $^{31}P^{31}P$ coupling constants are mostly "through-bond" in nature. On the contrary, for the nickel complexes, a dependence of $J_{PP'}$ on the P···P internuclear distances is observed (for d P···P = 3.765 Å, $J_{PP'}$ = 0 Hz, and for d P···P = 3.002 Å, $J_{PP'}$ = 67 Hz). The $J_{PP'}$ = 0 Hz for a P···P = 3.765 Å and the very strong $^{31}P^{31}P$ coupling constants at short internuclear distances lead us to assume that, in the case of the nickel compounds **1b** and **2**, the "through-bond" contribution to the overall coupling is weak as compared to the "through-space" pathway.[23]

3.4.3. $^{31}P^{31}P$ Coupling in the Free Ligand $Fc(P)_4{}^tBu$. According to the extended overlap interaction formulation, the free ligand $Fc(P)_4{}^tBu$ should be treated differently from the coordination complexes thereof. The X-ray structure of the

(22) For simplicity, we ignore the complete treatment of the molecular orbitals of the coordination complexes, including all of the metal and ancillary ligand orbitals.

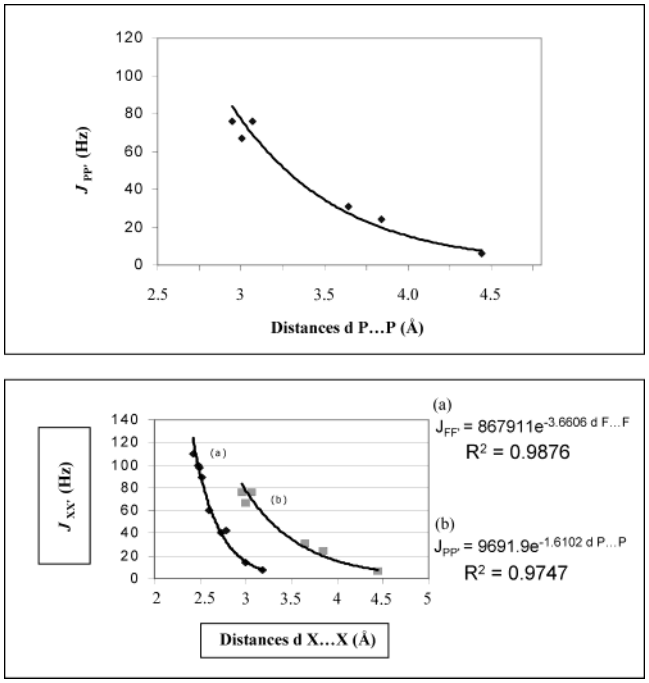

Figure 5. (Top) Plot of $J_{PP'}$ against *d* P···P using data from Table 1 related to the **1b**, **2**, and **3** metal complexes. The data are fitted by the exponential relationship defined by eq 2. (Bottom) Same data as in graph (b), as compared to data extracted from ref 25 in graph (a) related to the "through-space" $J_{FF'}$ coupling in organic compounds (curve-fitting program Excel 2000).

$Fc(P)_4{}^tBu$ ligand[5a] indicates that the P_1 and P_2 lone-pairs clearly point toward each other, suggesting a significant overlap and thus coupling pathway, in line with Mallory's formulation. In the case discussed above, the overlap between the bonding $M-P_1$ orbital and the P_4 lone-pair is much less directional, and thus less effective, leading to smaller "through-space" coupling constants. This is consistent with the strong nonbonded coupling constant $J_{PP'} = 60$ Hz observed for a distance *d* P···P = 3.73 Å in $Fc(P)_4{}^tBu$, while at such internuclear distances in the metal complexes, the corresponding $J_{PP'}$ values range between 20 and 30 Hz.

3.4.4. Quantitative Correlation of the Distance Dependence of $^{31}P^{31}P$ Coupling in Coordination Complexes. We have constructed the plot displayed in Figure 5 (top) using the data collected in Table 1. For the reasons outlined above, the data from the ligand $Fc(P)_4{}^tBu$ and from the homoannular phosphorus couplings in the palladium complexes **3** and **4** were excluded. On the other hand, the data from homoannular phosphorus in the nickel species, which do depend on phosphorus distances, were included. The data points were plotted $J_{PP'}$ versus d P···P. The best fit was obtained for an exponential curve expressed by eq 2, in which $J_{PP'}$ is in units of hertz and *d* P···P is in units of angstroms.[24]

$$J_{PP'} = (9691.9)e^{-1.6102d_{P\cdots P}} \qquad (2)$$

The regression coefficient for this curve, $R^2 = 0.975$, falls short of providing a definitive quantitative demonstration of the extended lone-pair overlap interaction model. However, this curve is overall consistent with the reported results concerning $^{19}F^{19}F$ nonbonded interactions.[10h,12a,25] It should be emphasized that the fitted data all correspond to experimentally obtained values, which span a wide range of coupling constants (from 6 to 76 Hz) as well as a wide range of distances (from 2.9 to 4.4 Å). For comparison, Figure 5 (bottom) displays the fitted $^{19}F^{19}F$ versus *d* F···F data previously reported by Ibrom and Ernst ($R^2 = 0.987$ with the distances computed with MM2).[25] We note for phosphorus (due to larger valence orbitals) detectable coupling constants corresponding to longer "through-space" distances. We note also a less steep exponential inverse dependence on internuclear distances, which we attribute to a less efficient orbital overlap.

Further improvements of the current model[26] should take into account the nature of the metal, as well as the weak "through-bond" coupling for homoannular phosphorus $^3J_{PP'}$ values.[11c] As was previously noted for J_{FF} coupling constants,[25] phosphorus nuclear spin−spin "through-space" interactions are detected for distances longer than the sum of van der Waals radii for phosphorus (3.6 Å).[27] While the semiquantitative experimental formulation presented herein is very convenient (as it presents an intuitive correlation between "geometric parameters" and "through-space" nucleus spin-coupling), a more significant correlation should probably be expressed in terms of orbitals overlap, taking into account the shape and the relative diffuse character of the electronic clouds. Consequently, further improvements will include quantitative orbital overlap effectiveness derived from molecular orbital calculations.

4. Summary

Both from a theoretical and from an experimental point of view, the analysis of high-resolution NMR parameters is a critical issue. A deeper understanding of the relationship between coupling constants and molecular structure could greatly broaden future applications of high-resolution spectroscopy for the elucidation of molecular structures.[28] Besides the theoretical computational studies on nuclear spin−spin transmission, concerning specifically "through-space" coupling constants, the previous works have focused on fluorine- and nitrogen-containing organic compounds with atoms having two lone-pair orbitals interacting. The present paper provides experimental

(23) Opposite results are found with palladium and nickel complexes for distances of about 3 Å. An explanation might be proposed if is taken into account that a contribution from metal is expected also when a lateral "through-space" coupling process is involved. Thus, while the valence orbitals of Ni are more contracted as compared to Pd orbitals, the Ni orbitals are much less diffuse, and their contribution to the nonbonded coupling should be, as well, "less diffuse". The consequence would be that, at short P internuclear distances, a nonbonded lateral orbital interaction would be more effective for Ni species than for Pd species as soon as metal orbitals are involved.

(24) In the reference work on fluorine-containing compounds (for instance, ref 10h), the dependence of J_{FF} on the extent to which the two lone-pair orbitals interact because of their overlap is directly proportional to the energy difference $\Delta E(\sigma_{FF}/\sigma_{FF}^*)$ (Scheme 4). In turn, this predicted dependence of J_{FF} on the extent of the lone-pair overlap suggests that J_{FF} should fall off exponentially with the distance between the two fluorines *d* F···F.

(25) Ernst, L.; Ibrom, K. *Angew. Chem., Int. Ed. Engl.* **1995**, *34*, 1881. In this communication devoted to "through-space" J_{FF} coupling constants in difluorocyclophane, the authors underline the discrepancy between the experimental values obtained for J_{FF} as a function of *d* F···F and some previous theoretical reports.

(26) One should be aware, as well, of the solvent dependence of the "through-space" coupling constant. In the present work, however, this is of no concern as $CDCl_3$ and CD_2Cl_2 were used throughout and similar values were consistently obtained. For a relevant study on the solvent effects in nonbonded J_{CF} and J_{HF}, see: Mele, A.; Vergani, B.; Viani, F.; Meille, S. V.; Farina, A.; Bravo, P. *Eur. J. Org. Chem.* **1999**, *187*, 7.

(27) (a) Bondi, A. *J. Phys. Chem.* **1964**, *68*, 441. (b) Pauling, L. *The Nature of the Chemical Bond*; Cornell University Press: Ithaca, NY, 1945.

(28) For convincing examples of structural determination using nonbonded spin−spin couplings, see: (a) Kimber, B. J.; Feeney, J.; Roberts, G. C. K.; Birdsall, B.; Griffiths, D. V.; Burgen, A. S. V.; Sykes, B. D. *Nature* **1978**, *271*, 184−185. (b) Albéniz, A. C.; Casado, A. L.; Espinet, P. *Organometallics* **1997**, *16*, 5416.

evidence and numerical values, potentially useful both to theoretical and to experimental chemists.[25] It provides a rationale to the variety of coupling constants observed between phosphorus atoms which are the result of nonbonded interaction. To the best of our knowledge, it is shown for the first time that only one lone-pair orbital which interacts with a bonding orbital can transfer the $^{31}P^{31}P$ nuclear spin information "through-space" between two phosphorus nuclei in a coordination complex.

Acknowledgment. We thank Thomas R. Ward, Anthony Vion, Sylviane Royer, and Geneviève Delmas for their kind help. We also thank the "Conseil Régional de Bourgogne" for a postdoctoral grant to V.V.I.

Supporting Information Available: Simulated ^{31}P NMR spectra for **1b**, **2**, and **4**, and full X-ray structural data for **1b** and **2** (CIF). This material is available free of charge via the Internet at http://pubs.acs.org.

JA048907A